

Wigner $6j$ symbols for $SU(N)$: Symbols with at least two quark-lines

Judith Alcock-Zeilinger,^{1,2} Stefan Keppeler,² Simon Plätzer,^{3,4,1} and Malin Sjodahl^{5,1}

¹⁾*Erwin Schrödinger Institute for Mathematics and Physics,*

University of Vienna, Boltzmannngasse 9, A-1090 Wien,

Austria

²⁾*Fachbereich Mathematik, Universität Tübingen, Auf der Morgenstelle 10,*

72076 Tübingen, Germany

³⁾*Institute of Physics, NAWI Graz, University of Graz, Universitätsplatz 5,*

A-8010 Graz, Austria

⁴⁾*Particle Physics, Faculty of Physics, University of Vienna, Boltzmannngasse 5,*

A-1090 Wien, Austria

⁵⁾*Department of Astronomy and Theoretical Physics, Lund University, Box 43,*

221 00 Lund, Sweden

(Dated: 29 September 2022)

We study a class of $SU(N)$ Wigner $6j$ symbols involving two fundamental representations, and derive explicit formulae for all $6j$ symbols in this class. Our formulae express the $6j$ symbols in terms of the dimensions of the involved representations, and they are thereby functions of N . We view these explicit formulae as a first step towards efficiently decomposing $SU(N)$ color structures in terms of group invariants.

I. INTRODUCTION

A unique feature of the characteristic quantum numbers of the strong force as described by Quantum Chromodynamics (QCD) is that they are confined and not observable. In order to extract observable quantities from QCD scattering amplitudes one has to average over external color quantum numbers or, otherwise, project onto definite hadronic states. In both cases the color quantum numbers enter calculations on a similar footing as internal interfering quantum mechanical degrees of freedom. This allows for the usage of color bases which leave out information on the states within an irreducible representation (irrep) of $SU(3)$.

Despite this simplification, one of the challenges in multi-parton QCD calculations is the accurate description of the large color space. Often color-summed/-averaged so-called trace¹⁻¹¹ and color-flow bases¹²⁻¹⁸ are used. These bases take advantage of the possibility to ignore the internal structure of $SU(3)$ irreps, but they also ignore the irreps altogether, i.e. the basis vectors are in no correspondence to the intermediate states in which a set of partons transforms. Moreover, for a finite number N of colors, trace and color-flow bases are non-orthogonal and overcomplete, i.e., strictly speaking, they are not even bases but only spanning sets. The size of these spanning sets grows roughly as a factorial in the number $n_{g+q\bar{q}}$ of gluons and $q\bar{q}$ -pairs¹⁹. Since these spanning sets are non-orthogonal, this translates, in the worst case, to a factorial square scaling, $(n_{g+q\bar{q}}!)^2$, for the number of inner products that have to be calculated. In a full color description of a scattering cross section this growth will be prohibitive if one calculates all contributing terms and cannot use additional information about the amplitudes or exploit Monte Carlo methods to sample over color structures, as *e.g.* done in¹⁷.

An ideal basis would be both orthogonal and minimal, allowing for the smallest number of terms needed when expanding amplitudes and correlation functions in color structures. These properties are combined in multiplet bases¹⁹⁻³⁰, which use representation theory to iteratively group partons into orthogonal states. So far, the use of multiplet bases has been rather limited, in part likely due to the lack of explicit bases for many partons, i.e. *the* situation in which they would really be advantageous.

In this paper we suggest taking the usage of representation theory one step further: Instead of *explicitly* created bases, we advocate using Wigner $6j$ coefficients (or $6j$ symbols

or just $6js$ – we use all these terms interchangeably in this paper) for calculations in color space. This, however, assumes that the required $6j$ coefficients have been calculated and are readily available also for a high number of partons. In Refs. 25,30 explicit bases were used to calculate $6js$ for a limited number of partons. This allows for a fast decomposition at use-time, i.e. when the $6js$ (corresponding to the same bases) are used in actual computations of amplitudes, but the factorial growth of the spanning set remains a challenge at construction time, thereby effectively limiting the number of involved particles to one or a few handfuls.

When decomposing color structures into multiplet bases using $6js$, no explicit bases are needed; i.e. all calculations are performed in terms of $SU(N)$ group invariant $6j$ coefficients, along with dimensions of representations and Wigner $3j$ coefficients (or $3j$ symbol, or $3j$ for short), which may be normalized to 1. This poses the question if it should not also be possible to derive these invariants in terms of themselves. More precisely: Can one derive a consistent set of $6j$ coefficients only in terms of group invariants, specifically the dimensions of representations?

In this paper we answer this question affirmatively when at least two of the irreps involved in a $6j$ symbol are fundamental representations, i.e. quark-lines, that do not share a common vertex. In [Theorem 1](#) we present explicit formulae for the absolute values of all $6j$ symbols in this class. We also explain how to iteratively fix and determine the signs of these $6js$, and for $N \leq 3$ we prove (whereas for $N > 3$ we conjecture) that this procedure always leads to a consistent set of signs. In particular, we have thus determined these $6j$ symbols in the phenomenologically relevant case $N = 3$. For $N = 2$ the problem was generally solved before, see e.g. Ref. 31. In future work we will show how to determine the other $6js$ required for a full color decomposition. We note that other approaches for calculating $SU(3)$ $6js$ in terms of Clebsch-Gordan coefficients exist^{32,33}, but stress that our method exploits group invariants *only*.

We view our results as a first step towards a complete reduction of color space in terms of $SU(N)$ group invariants, which has the potential to significantly simplify fixed-order as well as all-order calculations in color space, ranging from analytic approaches up to Monte Carlo methods. The reduction of color space in terms of invariants also has the potential to provide further insight into other aspects such as the color structure of hadronization models^{34,35}.

This paper is organized as follows: [Section II](#) gives a brief introduction to the birdtrack

method for $SU(N)$, illustrating how $6j$ symbols appear and how they can be used to decompose more general color structures. In [Section III](#) we introduce the particular class of $6j$ symbols of interest to the present paper, and in [Section IV](#) we describe properties of general $6j$ symbols, as well as of the class of symbols studied here. [Section V](#) constitutes the main part of this paper, wherein the closed form expressions of the $6j$ s are presented in [Theorem 1](#). The relevance of these results, as well as future work complementing them, are discussed in [Section VI](#).

II. BIRDTRACK METHODS FOR $SU(N)$ COLOR SPACE

In this section we briefly outline how to utilize the birdtrack method for decomposing group invariant (color) structures in terms of dimensions, Wigner- $3j$ and Wigner- $6j$ symbols. For a full, comprehensive introduction to the birdtrack formalism, readers are referred to [Ref. 36](#). The hasty reader finds a minimal introduction in [Appendix A](#) of [Ref. 19](#), whereas a more pedagogical account can be found in [Ref. 37](#). Examples of birdtrack calculations for QCD can be found in [Ref. 24,25](#).

We start out with a reminder that implicit indices of states within a representation are always summed over. We therefore have, for an irrep α ,

$$\begin{array}{c} \alpha \\ \circlearrowleft \\ \circlearrowright \end{array} = d_\alpha, \quad (1)$$

i.e. the sum of states within an irrep adds up to the dimension d_α of that irrep.

The second simplest color structure that may be encountered, which also contains a sum, is the “self energy” diagram

$$\begin{array}{c} \alpha \\ \parallel \\ \circlearrowleft \\ \delta \\ \circlearrowright \\ \parallel \\ \beta \end{array} = \frac{\begin{array}{c} \gamma \\ \circlearrowleft \\ \delta \\ \circlearrowright \end{array}}{d_\alpha} \parallel \begin{array}{c} \alpha \\ \parallel \\ \beta \end{array}, \quad (2)$$

where the free line is to be understood as a Kronecker delta in the representation indices α and β , and the normalization constant can be found by contracting indices on both sides;

as a consistency check, we have

Equation (3) shows a diagrammatic identity. On the left, a loop with two internal lines is shown. The top line is labeled α and $\beta = \alpha$, and the bottom line is labeled δ . A small loop is attached to the top line, labeled γ . This is equal to the fraction $\frac{\text{3j symbol}}{d_\alpha} d_\alpha$, which simplifies to the 3j symbol. The 3j symbol is a circle with a horizontal line through it, labeled δ above and α below, and a γ label above the circle.

where we used Equation (1). The result on the right hand side is known as a $3j$ symbol. It is proportional to the magnitude of the vertex, and, depending on the vertex normalization, it may thus assume different values. We will keep the normalization of the $3j$ symbol arbitrary for most of our derivations, although our final results are stated in the normalization where all $3j$ s are normalized to 1. This is in contrast to the standard QCD normalization for which, for example $\text{tr}[\text{oooo}] = \frac{1}{2}(N^2 - 1)$, for the generator normalization $\text{tr}[t^a t^b] = \frac{1}{2}\delta^{ab}$.

After the self-energy, with the topology of a loop involving two internal representations, the next structure to consider is the vertex correction. Here, we also encounter the Wigner- $6j$ symbols for the first time, as they act as normalization constants when eliminating loops with three internal lines,

Equation (4) shows a diagrammatic identity. On the left, a vertex correction diagram is shown with three external lines labeled α , σ , and ρ , and three internal lines labeled β , γ , and δ . This is equal to a sum over a of $\frac{1}{\text{loop}} \times \text{Wigner-6j symbol} \times \text{vertex}$. The loop is a circle with a horizontal line through it, labeled α above and ρ below, and a σ label above the circle. The Wigner-6j symbol is a triangular pictogram with three internal lines labeled α , β , and γ , and three external lines labeled σ , ρ , and δ . The vertex is a triangle with three external lines labeled α , σ , and ρ .

where the sum over all possible vertices a collapses to only one term if the irreps α , σ and ρ admit only one vertex. For the particular $6j$ symbols discussed in this paper, this is always the case. The triangular pictogram in Equation (4) describes a Wigner- $6j$ symbol which, in the case of $SU(2)$, is usually denoted in 2-line notation as

Equation (5) shows the 2-line notation for the Wigner-6j symbol. The triangular pictogram is shown on the left, and an arrow labeled $SU(2)$ points to the 2-line notation: $\left\{ \begin{matrix} j_\beta & j_\gamma & j_\alpha \\ j_\delta & j_\rho & j_\sigma \end{matrix} \right\}$.

For loops with more than three internal representations there is no similar simple expression. Instead, such color structures can be systematically reduced into loops with fewer

internal lines by the application of the completeness relation

$$= \sum_{\delta} \frac{d_{\delta}}{\beta} \begin{array}{c} \beta \\ \gamma \end{array} \begin{array}{c} \beta \\ \gamma \end{array} \quad (6)$$

Applying this to a loop with more internal irreps, the color structure can be rewritten in terms of a shorter loop and a sum of vertex corrections, which may be removed using Equation (4). Schematically, we have

$$\begin{array}{c} \text{Hexagon with red lines} \end{array} \stackrel{(6)}{=} \sum_{\alpha} \frac{d_{\alpha}}{\ominus} \begin{array}{c} \text{Hexagon with red line and circle} \end{array} \stackrel{(4)}{=} \sum_{\alpha} \frac{d_{\alpha}}{\ominus \ominus} \begin{array}{c} \text{Hexagon with red line and triangle} \end{array}, \quad (7)$$

which can be fully reduced to $3j$ s, $6j$ s and dimensions by applying the completeness relation two more times. In a similar fashion, loops with yet more internal representations can be reduced back to expressions involving dimensions and $3j$ and $6j$ coefficients.

For this reason, to decompose an arbitrary color structure into group invariants, it is in principle enough to know the dimensions which may be calculated using standard methods (see e.g. ^{36,38,39}, also summarized in Appendix E), the $3j$ coefficients (which we normalize via the vertices to 1) and the $6j$ coefficients, a class of which will be derived here.

III. WIGNER- $6j$ SYMBOLS WITH TWO OPPOSING QUARK-LINES

In this work we focus on $6j$ symbols with (at least) two quark-lines on opposite edges,

$$\begin{array}{c} \text{Triangle with edges } M_i, M_j, M^{ij} \text{ and internal lines } \alpha \end{array}, \quad (8)$$

where the single lines are understood to be in the fundamental representation, and α , M_i , M_j and M^{ij} are irreps which can be thought about as Young diagrams. For the main part

of this paper, we will assume that none of the irreps labeled by α , M_i , M_j and M^{ij} is the fundamental representation, as this allows us to ignore irrep ordering in vertices (this is explained in detail in [Appendix C](#)). However, [Appendix D](#) discusses a few special cases where some of these irreps are indeed the fundamental representation corresponding to \square .

The Young diagrams α , M_i , M_j and M^{ij} used in the construction of the $6j$ symbol given in [Equation \(8\)](#) are related to each other as follows:

- We begin by fixing a Young diagram α .
- Thereafter, we add a single box to α in row i (resp. j) in order to obtain M_i (resp. M_j). Note that, in general, we cannot add a box to every row of α since in some cases the result would not be a Young diagram.
- Lastly, M^{ij} is the diagram obtained from α by adding two boxes, first one in row i and then one in row j . If M_i and M_j both exist, then the final result of adding two boxes is commutative, i.e.

$$M^{ij} = M^{ji} . \quad (9)$$

Examples for the construction of M_i , M_j and M^{ij} from a fixed diagram α are given in [Figure 1](#).

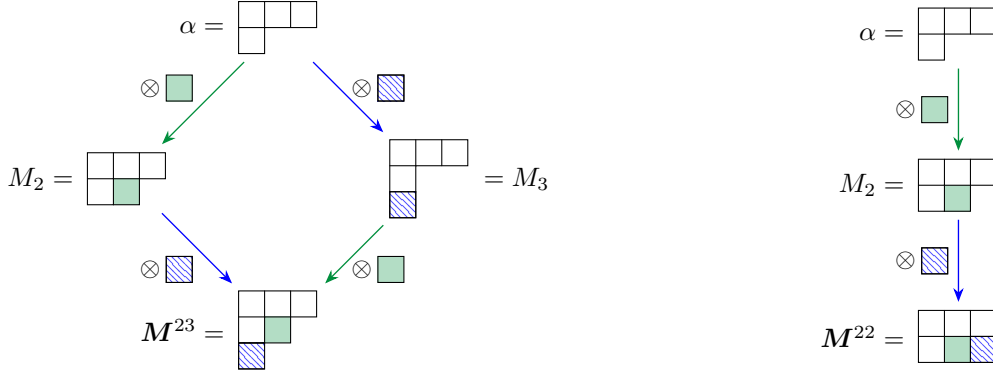
We denote the dimensions of the irreps corresponding to α , M_i , M_j and M^{ij} by d_α , d_i , d_j , and d_{ij} , respectively,

$$\dim(\alpha) = d_\alpha , \quad \dim(M_i) = d_i , \quad \dim(M_j) = d_j \quad \text{and} \quad \dim(M^{ij}) = d_{ij} . \quad (10)$$

These dimensions can be calculated with standard methods from the corresponding diagrams, see [Appendix E](#).

Since the $6j$ symbols discussed in this paper have the property that the two fundamental lines and the irrep indexed by α are fixed, we may denote the $6j$ symbol in [Equation \(8\)](#) by $S_{i,j}^{ij}$, where the bottom two indices i, j correspond to the indices of the two diagrams M_i and M_j , and the upper double-index corresponds to the double-index of the diagram M^{ij} ,

$$S_{i,j}^{ij} = \begin{array}{c} \text{Diagram} \end{array} . \quad (11)$$



(a) For $i = 2$ and $j = 3$, we obtain M_2 , M_3 and M^{23} from α by adding a green (shaded) box in row 2 and a blue (hatched) box in row 3. (b) For $i = j = 2$ we obtain M_2 and M^{22} from α by adding both boxes in row 2.

FIG. 1: Two examples constructing M_i , M_j and M^{ij} from the Young diagram $\alpha = \begin{array}{|c|c|c|} \hline \square & \square & \square \\ \hline \end{array}$ for different values of i and j .

It should be noted that the irrep M^{ii} (both indices equal), provided it is admissible, is contained in the product $M_j \otimes \square$ if and only if $j = i$, as is also illustrated in Figure 1b. Thus,

for fixed M^{ii} :
$$S_{a,b}^{ii} = \delta_{ia}\delta_{ib} \begin{array}{c} \begin{array}{c} \alpha \\ \nearrow M_a \\ \searrow M_b \\ \text{---} M^{ii} \end{array} \end{array}, \quad (12)$$

and, similarly,

for fixed M^{ij} :
$$S_{i,b}^{ij} = \delta_{jb} \begin{array}{c} \begin{array}{c} \alpha \\ \nearrow M_i \\ \searrow M_b \\ \text{---} M^{ij} \end{array} \end{array}. \quad (13)$$

Conversely, if we fix the diagrams M_i and M_j , the only irrep labeled by M^{ab} that would render the $6j$ symbol $S_{i,j}^{ab}$ nonzero is precisely that corresponding to M^{ij} ,

for fixed M_i and M_j :
$$S_{i,j}^{ab} = \delta_{ia}\delta_{jb} \begin{array}{c} \begin{array}{c} \alpha \\ \nearrow M_i \\ \searrow M_j \\ \text{---} M^{ab} \end{array} \end{array}, \quad (14)$$

and, if $i = j$,

$$\text{for fixed } M_i \quad \mathcal{S}_{i,i}^{ab} = \delta_{ia} \quad \begin{array}{c} \text{Diagram: A triangle with vertices at the top, bottom-left, and bottom-right. The top edge is a blue line with an arrow pointing right, labeled } M_i. \text{ The bottom-left edge is a green line with an arrow pointing right, labeled } M_i. \text{ The bottom-right edge is a red line with an arrow pointing right, labeled } M^{ab}. \text{ An orange arrow labeled } \alpha \text{ points vertically upwards from the bottom edge to the top vertex.} \end{array} \quad . \quad (15)$$

We remark that the $6j$ symbol in Equation (8) is actually the most general $6j$ containing two quark-lines not meeting in one vertex: Even though one might suspect that flipping the direction of one or several arrows would lead to further $6j$ symbols, this is not the case as can be deduced from the discussion in Section IV C. The full set of $6js$ with two or more quark-lines will, in addition, contain $6js$ where two quark-lines meet in one vertex. The cases in which both quark-lines are incoming or in which both quark-lines are outgoing in a vertex are discussed in Appendix D. If one of the two quark-lines meeting in a vertex is incoming and the other is outgoing, we have to distinguish two cases: Either the two lines form a singlet (trivial representation), in which case the $6j$ is reduced to a $3j$ (up to normalization), or they are in the adjoint representation, i.e. forming a gluon-line. The latter case will be discussed in a future publication, together with other $6j$ symbols containing gluon-lines. The class of $6js$ defined by (8) is one that is often encountered in a QCD context, cf. Ref. 30, Equations. (2.7) and (2.8). In future work we will study the remaining $6js$ needed to decompose color structure, as well as their applications to QCD.

Before we derive relations between $6j$ symbols of the form (8) in Section V A, we require some more properties of these symbols, which will be discussed in the following Section IV.

IV. PROPERTIES OF $6j$ SYMBOLS

The present section discusses several properties of $6j$ symbols that will be used in this paper. First, we briefly discuss irrep line orderings in vertices in Section IV A. Section IV B focuses on symmetries of $6j$ symbols, where we, in particular, make use of the fact that a $6j$ symbol in its graphical representation can be viewed as a tetrahedron. In Section IV C we restrict ourselves to the $6j$ symbols of interest in this paper (i.e. those defined in Section III) and discuss additional symmetries that arise from having two fundamental representations on opposite edges of the $6j$.

A. Line ordering in vertices

In birdtrack calculations we may end up with diagrams that are complicated to read because of (unnecessary) line crossings. In such cases it is convenient to introduce barred vertices, indicating that two lines in a vertex have been swapped, i.e. we define

$$\begin{array}{c} \beta \swarrow \quad \nearrow \alpha \\ \downarrow \gamma \end{array} = \begin{array}{c} \beta \swarrow \quad \nearrow \alpha \\ \downarrow \gamma \end{array} . \quad (16)$$

Fortunately, for most vertices appearing in this work, the bars can be omitted again in the next step as we explain in [Appendix C](#). The only vertex relevant for this work for which line swapping leads to a phase change is the vertex that is used for the antisymmetric projection of two quark-lines, for which we have

$$\begin{array}{c} \beta \swarrow \quad \nearrow \alpha \\ \downarrow \gamma \end{array} = - \begin{array}{c} \beta \swarrow \quad \nearrow \alpha \\ \downarrow \gamma \end{array} . \quad (17)$$

However, since there are only a few $6j$ symbols satisfying the conditions laid out in [Section III](#) that also contain the vertex in [Equation \(17\)](#), we discuss these separately in [Appendix D](#), and assume for the remainder of this paper that all vertices appearing in the $6j$ symbols in question are equal to their barred counterparts,

$$\begin{array}{c} \beta \swarrow \quad \nearrow \alpha \\ \downarrow \gamma \end{array} = \begin{array}{c} \beta \swarrow \quad \nearrow \alpha \\ \downarrow \gamma \end{array} \quad \text{if } \alpha \neq \beta \neq \gamma \neq \alpha . \quad (18)$$

B. Symmetries of general $6j$ symbols

A Wigner- $6j$ symbol in its graphical *birdtrack* form may be thought of as a tetrahedron, where our usual notation represents a top-down planar projection. For example, for a $6j$ symbol connecting general irreps $\alpha, \beta, \gamma, \delta, \rho$ and σ ,

$$\begin{array}{c} 4 \\ \beta \swarrow \quad \nearrow \alpha \\ \sigma \swarrow \quad \nearrow \rho \\ \delta \swarrow \quad \nearrow \gamma \\ 1 \quad \quad \quad 2 \quad 3 \end{array} \xrightarrow{\text{top-down projection}} \begin{array}{c} 3 \\ \sigma \swarrow \quad \nearrow \rho \\ \alpha \swarrow \quad \nearrow \gamma \\ \beta \swarrow \quad \nearrow \delta \\ 1 \quad \quad \quad 2 \quad 4 \end{array} , \quad (19)$$

where we have labeled the vertices of the tetrahedron and the corresponding $6j$ as 1, 2, 3, 4 for visual clarity. Clearly, which of the four vertices of the tetrahedron we view as the top

vertex is a completely arbitrary choice and thus cannot affect the $6j$ symbol in any way. Therefore, we find that

$$\begin{array}{c}
 \begin{array}{c} 3 \\ \downarrow \alpha \\ \begin{array}{ccc} \sigma \nearrow & 4 & \rho \nearrow \\ \beta \nearrow & & \gamma \nearrow \\ \delta \rightarrow & & \end{array} \\ \begin{array}{ccc} 1 & & 2 \end{array} \end{array} = \begin{array}{c} 4 \\ \uparrow \beta \\ \begin{array}{ccc} \alpha \nearrow & 1 & \gamma \nearrow \\ \delta \rightarrow & & \rho \rightarrow \\ \sigma \rightarrow & & \end{array} \\ \begin{array}{ccc} 3 & & 2 \end{array} \end{array} = \begin{array}{c} 4 \\ \uparrow \gamma \\ \begin{array}{ccc} \beta \nearrow & 2 & \alpha \nearrow \\ \delta \rightarrow & & \rho \rightarrow \\ \sigma \rightarrow & & \end{array} \\ \begin{array}{ccc} 1 & & 3 \end{array} \end{array} = \begin{array}{c} 4 \\ \uparrow \alpha \\ \begin{array}{ccc} \gamma \nearrow & 3 & \beta \nearrow \\ \delta \rightarrow & & \rho \rightarrow \\ \sigma \rightarrow & & \end{array} \\ \begin{array}{ccc} 2 & & 1 \end{array} \end{array} . \quad (20a)
 \end{array}$$

By that same token, a rotation by 60° also leaves the $6j$ symbol unchanged,

$$\begin{array}{c}
 \begin{array}{c} 3 \\ \downarrow \alpha \\ \begin{array}{ccc} \sigma \nearrow & 4 & \rho \nearrow \\ \beta \nearrow & & \gamma \nearrow \\ \delta \rightarrow & & \end{array} \\ \begin{array}{ccc} 1 & & 2 \end{array} \end{array} = \begin{array}{c} 2 \\ \downarrow \gamma \\ \begin{array}{ccc} \rho \nearrow & 4 & \delta \nearrow \\ \alpha \nearrow & & \beta \nearrow \\ \sigma \rightarrow & & \end{array} \\ \begin{array}{ccc} 3 & & 1 \end{array} \end{array} = \begin{array}{c} 1 \\ \downarrow \beta \\ \begin{array}{ccc} \delta \nearrow & 4 & \sigma \nearrow \\ \gamma \nearrow & & \alpha \nearrow \\ \rho \rightarrow & & \end{array} \\ \begin{array}{ccc} 2 & & 3 \end{array} \end{array} . \quad (20b)
 \end{array}$$

C. Symmetry properties of $6j$ symbols with two quark-lines

In the present paper, we want to focus on $6j$ symbols that were described in [Section III](#),

$$\begin{array}{c}
 \begin{array}{c} 4 \\ \downarrow \alpha \\ \begin{array}{ccc} \beta \nearrow & & \gamma \nearrow \\ \sigma \nearrow & & \rho \nearrow \\ \delta \rightarrow & & \end{array} \\ \begin{array}{ccc} 1 & & 2 \end{array} \end{array} \xrightarrow{\text{specialize to}} \begin{array}{c} 4 \\ \downarrow \alpha \\ \begin{array}{ccc} M_j \nearrow & & \nearrow \\ M_i \nearrow & & \nearrow \\ M^{ij} \rightarrow & & \end{array} \\ \begin{array}{ccc} 1 & & 2 \end{array} \end{array} , \quad (21)
 \end{array}$$

which affords us additional symmetries. Firstly, since the two quark-lines (the blue and green single lines) are both in the *fundamental* representation, we may “exchange” them without changing the $6j$ symbol,

$$S_{i,j}^{ij} = \begin{array}{c} \begin{array}{c} 4 \\ \downarrow \alpha \\ \begin{array}{ccc} M_j \nearrow & & \nearrow \\ M_i \nearrow & & \nearrow \\ M^{ij} \rightarrow & & \end{array} \\ \begin{array}{ccc} 1 & & 2 \end{array} \end{array} = \begin{array}{c} \begin{array}{c} 4 \\ \downarrow \alpha \\ \begin{array}{ccc} M_j \nearrow & & \nearrow \\ M_i \nearrow & & \nearrow \\ M^{ij} \rightarrow & & \end{array} \\ \begin{array}{ccc} 1 & & 2 \end{array} \end{array} ; \quad (22)
 \end{array}$$

we will, however, continue to draw the two quark-lines in different colors for visual clarity, as this will make the discussions that follow (in particular those of [Appendix A](#)) more legible.

Consider $S_{i,j}^{ab}$ corresponding to the last expression in [Equation \(20a\)](#) and exchange the green and blue fundamental lines according to [Equation \(22\)](#) to end up with the following

graphical form of $S_{i,j}^{ab}$,

$$S_{i,j}^{ab} = \begin{array}{c} \text{Diagram 1} \\ \xrightarrow{(20a)} \\ \text{Diagram 2} \\ \xrightarrow{(22)} \\ \text{Diagram 3} \end{array} . \quad (23a)$$

If we form the complex conjugate of this depiction of the $6j$ symbol (which, in the birdtrack formalism, is done by reversing all arrows and barring all vertices, cf. [Appendix C](#)), we will obtain a different $6j$ symbol, namely $S_{j,i}^{ab}$ (notice the order of the lower indices),

$$(S_{i,j}^{ab})^* = \left(\begin{array}{c} \text{Diagram 1} \\ \text{Diagram 2} \\ \text{Diagram 3} \end{array} \right)^* = \begin{array}{c} \text{Diagram 4} \\ \text{Diagram 5} \\ \text{Diagram 6} \end{array} = \begin{array}{c} \text{Diagram 7} \\ \text{Diagram 8} \\ \text{Diagram 9} \end{array} = S_{j,i}^{ab} , \quad (23b)$$

where we were able to ignore the bars on the vertices in the middle $6j$ symbol as we assume that all of its vertices obey [Equation \(18\)](#). (All $6j$ symbols encountered here, not satisfying this, are the ones involving [\(17\)](#). These are discussed separately in [Appendix D](#)).

It is easy to convince oneself that all $6j$ s naturally can be chosen to be real by writing out representations in terms of the fundamental representations and symmetrizers and anti-symmetrizers. Contracting all quark-lines yields a real polynomial in N , such that $S_{i,j}^{ab} \in \mathbb{R}$, and it follows that $(S_{i,j}^{ab})^* = S_{i,j}^{ab}$, and hence

$$S_{i,j}^{ab} = S_{j,i}^{ab} . \quad (24)$$

In conclusion, for fixed i, j with $i \neq j$, there are four distinct types of $6j$ symbols, namely

$$\begin{array}{cccc} S_{i,i}^{ii} & S_{i,i}^{ij} & S_{j,j}^{ij} & S_{i,j}^{ij} = S_{j,i}^{ij} \\ \parallel & \parallel & \parallel & \parallel \\ \text{Diagram 1} & \text{Diagram 2} & \text{Diagram 3} & \text{Diagram 4} \end{array} . \quad (25)$$

In the following [Section V](#) we proceed to first derive relations between these four $6j$ symbols, and then solve this system of equations to obtain their closed form expressions.

V. CLOSED FORM EXPRESSIONS OF $6j$ SYMBOLS

In the present section, we present several relations between the four $6j$ symbols given in Equation (25). In Section VB, we use these relations to find closed form expressions of the $6j$ symbols. These expressions are summarized in Theorem 1, which is the main result of this paper.

A. Relations between $6j$ symbols

Through the repeated use of the completeness relation Equation (6) and the vertex correction Equation (4), we find the following relations between the four distinct $6j$ symbols given in Equation (25) (the derivations can be found in Appendix A):

1. For a given representation \mathbf{M}^{ij} , we obtain

$$1 = (d_i)^2 (S_{i,i}^{ij})^2 + d_i d_j (S_{i,j}^{ij})^2 . \quad (26a)$$

Furthermore,

$$0 = d_i S_{i,i}^{ij} S_{i,j}^{ij} + d_j S_{i,j}^{ij} S_{j,j}^{ij} . \quad (26b)$$

2. For two given representations \mathbf{M}_i and \mathbf{M}_j , we obtain

$$\frac{1}{d_\alpha} = \sum_{\mathbf{M}^{ab}} d_{ab} (S_{i,j}^{ab})^2 , \quad (26c)$$

where d_{ab} is the dimension of the representation \mathbf{M}^{ab} .

3. For a given representation \mathbf{M}_i , we have

$$1 = \sum_b d_{ib} S_{i,i}^{ib} . \quad (26d)$$

Notice that, in these relations, all $3j$ symbols were set to 1; the derivations in Appendix A keep all $3j$ s explicit until the very last step.

B. Solving for closed form expressions

In the present section, we derive closed form expressions for the $6j$ symbols using the relations presented in the previous Section VA. For the purpose of this section, we assume

that all the $6j$ s appearing in these relations are admissible (that is boxes can be added in rows i and j for the particular diagram α from which we start).

Let us start with [Equation \(26a\)](#) : Notice that, if we choose the representation \mathbf{M}^{ij} such that $i = j$, $\mathbf{M}^{ij} \rightarrow \mathbf{M}^{ii}$, the second term vanishes in accordance with [Equation \(12\)](#), such that [Equation \(26a\)](#) reduces to

$$\begin{aligned} \text{Equation (26a)} \quad & \xrightarrow{\mathbf{M}^{ij} \rightarrow \mathbf{M}^{ii}} \quad 1 = (d_i)^2 (S_{i,i}^{ii})^2 \\ & \iff S_{i,i}^{ii} = \pm \frac{1}{d_i} . \end{aligned} \quad (27)$$

In fact, in [Appendix B 1](#) we show that this $6j$ symbol is always positive, such that

$$S_{i,i}^{ii} = \frac{1}{d_i} . \quad (28)$$

If in [Equation \(26c\)](#) we instead choose $i \neq j$ (i.e. we choose M_i and M_j to be inequivalent), there is only one possible \mathbf{M}^{ab} that renders the $6j$ nonzero, namely \mathbf{M}^{ij} (this follows from condition (14)). Thus, the sum on the right hand side of [Equation \(26c\)](#) reduces to one term, allowing us to solve for yet another $6j$ symbol,

$$\begin{aligned} \text{Equation (26c)} \quad & \xrightarrow{i \neq j} \quad \frac{1}{d_\alpha} = d_{ij} (S_{i,j}^{ij})^2 \\ & \iff S_{i,j}^{ij} = \pm \frac{1}{\sqrt{d_\alpha d_{ij}}} . \end{aligned} \quad (29)$$

In [Appendix B 2](#) we explain how the overall sign of $S_{i,j}^{ij}$ can be chosen.

We may now plug the result for $S_{i,j}^{ij}$ back into the full form of [Equation \(26a\)](#) to also obtain a closed form expression for $S_{i,i}^{ij}$,

$$\begin{aligned} 1 = (d_i)^2 (S_{i,i}^{ij})^2 + d_i d_j (S_{i,j}^{ij})^2 & \xrightarrow{(S_{i,j}^{ij})^2 = \frac{1}{d_\alpha d_{ij}}} \quad 1 = (d_i)^2 (S_{i,i}^{ij})^2 + \frac{d_i d_j}{d_\alpha d_{ij}} \\ & \iff S_{i,i}^{ij} = \pm \frac{1}{d_i} \sqrt{1 - \frac{d_i d_j}{d_\alpha d_{ij}}} . \end{aligned} \quad (30)$$

Lastly, since by [Equation \(29\)](#) $S_{i,j}^{ij} \neq 0$, we may now derive the last $6j$ symbol, namely $S_{j,j}^{ij}$, using relation [\(26b\)](#):

$$\begin{aligned} 0 = d_i S_{i,i}^{ij} S_{i,j}^{ij} + d_j S_{j,j}^{ij} S_{i,j}^{ij} & = (d_i S_{i,i}^{ij} + d_j S_{j,j}^{ij}) S_{i,j}^{ij} \\ \xrightarrow{S_{i,j}^{ij} \neq 0} \quad d_j S_{j,j}^{ij} & = -d_i S_{i,i}^{ij} = \mp \sqrt{1 - \frac{d_i d_j}{d_\alpha d_{ij}}} . \end{aligned} \quad (31)$$

In [Appendix B 3](#) we show how the signs of $S_{i,i}^{ij}$ (and hence $S_{j,j}^{ij}$) can be uniquely determined from [Equation \(26d\)](#) for $N \leq 3$.

In summary:

Theorem 1 (Closed form expressions for the distinct $6j$ symbols) *For each of the distinct $6j$ symbols identified in [Equation \(25\)](#), we obtain the following closed form expression:*

$$S_{i,i}^{ii} = \frac{1}{d_i} \quad , \quad d_i S_{i,i}^{ij} = \pm \sqrt{1 - \frac{d_i d_j}{d_\alpha d_{ij}}} = -d_j S_{j,j}^{ij} \quad , \quad S_{i,j}^{ij} = \pm \frac{1}{\sqrt{d_\alpha d_{ij}}} \quad , \quad (32)$$

where the sign of the $S_{i,j}^{ij}$ depends on the definition of the vertices as discussed in [Appendix B 2](#). The signs of $S_{i,i}^{ij}$ (equivalently $S_{j,j}^{ij}$) can be uniquely determined from [Equation \(26d\)](#) for $N \leq 3$, cf. [Appendix B 3](#).

We remark that, with the above, the problem of calculating Wigner- $6j$ symbols with quark-lines on opposing edges has been reduced to finding the dimensions of the representations. Once these are known, given that a starting representation α results in a maximal number of new $6j$ symbols, the scaling of finding all relevant $6js$ (of the given form) with n boxes is therefore given by the number of possible representations α with $n-2$ boxes, which scales as n for $N=3$. This implies that finding all $6js$ with *up to* n boxes scales only as n^2 for $N=3$.

VI. CONCLUSIONS AND OUTLOOK

In this paper we have taken the first steps towards deriving Wigner $6j$ coefficients in terms of $SU(N)$ group invariants only by writing down closed form expressions of a set of $6js$ involving at least two fundamental representations.

We are presently supplementing this with a limited set of $6js$ involving the adjoint representation, which will be enough to allow for a complete color decomposition of amplitudes in QCD³⁰. While the $6js$ with two quark-lines are expressed in terms of dimensions only, the gluon $6js$ require the quark $6js$. Beyond this one may anticipate that yet more general $6js$ would be similarly expressible.

Once complemented with the gluon $6js$, we expect these sets of $6js$ to have significant phenomenological relevance by opening up, for the first time, the possibility to work with orthogonal physical states also for processes involving many partons.

ACKNOWLEDGMENTS

MS acknowledges support by the Swedish Research Council (contract number 2016-05996, as well as the European Union’s Horizon 2020 research and innovation programme (grant agreement No 668679). MS and SP have in part also been supported by the European Union’s Horizon 2020 research and innovation programme as part of the Marie Skłodowska-Curie Innovative Training Network MCnetITN3 (grant agreement no. 722104). JAZ is thankful to the Alexander von Humboldt Foundation for support via the Fellowship for Postdoctoral Researchers, as well as to the Erwin Schrödinger Institute for their support via the Junior Research Fellowship. This stay at ESI was essential for the completion of this work. We are also grateful to the Erwin Schrödinger Institute Vienna for hospitality and support while significant parts of this work have been started within the Research in Teams programme “Amplitude Level Evolution II: Cracking down on color bases” (RIT0521).

Appendix A: Relating different $6j$ symbols

In this appendix, we derive [Equations \(26a\) to \(26d\)](#), which were used to obtain the closed form expressions of the $6j$ symbols given in [Theorem 1](#). These derivations make extensive use of the birdtrack formalism introduced in [Section II](#).

1. Proof of [Equations \(26a\) and \(26b\)](#)

Let α be a particular Young diagram, and let M_i and M^{ij} be obtained from α in accordance with [Section III](#). Then, we may consider the following birdtrack diagram,


(A1)

We may insert a completeness relation (cf. Equation (6)) between α and the green (top) quark-line to obtain,

$$\text{Diagram} = \sum_b \frac{d_b}{\text{Diagram}} \text{Diagram}; \quad (\text{A2})$$

from this it is clear that the diagrams M_b are also obtained from α by adding a single box (corresponding to the top quark-line).

The vertex correction on the right-hand side of Equation (A2) gives rise to a $6j$ symbol (cf. Equation (4)),

$$\text{Diagram} = \frac{1}{\text{Diagram}} \text{Diagram}, \quad (\text{A3})$$

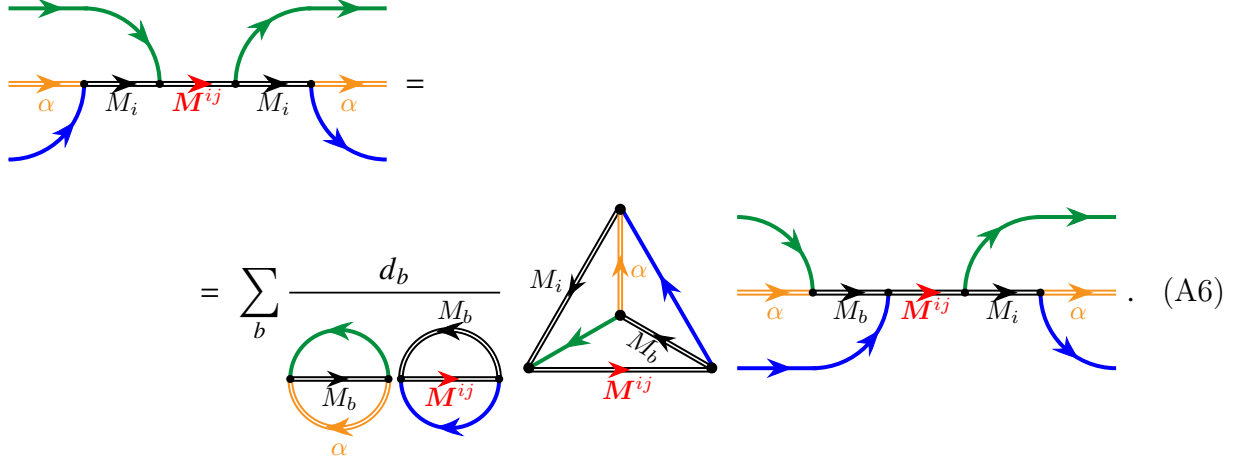
and allows us to rewrite Equation (A2) as

$$\text{Diagram} = \sum_b \frac{d_b}{\text{Diagram}} \text{Diagram}. \quad (\text{A4})$$

a. *Proof of Equation (26a)*: Consider the Hermitian conjugate of the expression in Equation (A1) (formed by flipping the birdtrack about the vertical axis and reversing all arrows, cf. Ref. 36),

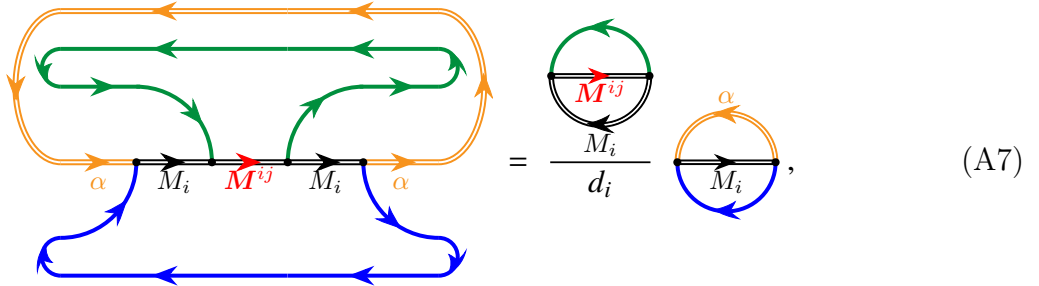
$$\left(\text{Diagram} \right)^\dagger = \text{Diagram}, \quad (\text{A5})$$

and multiply it from the right onto Equation (A4),



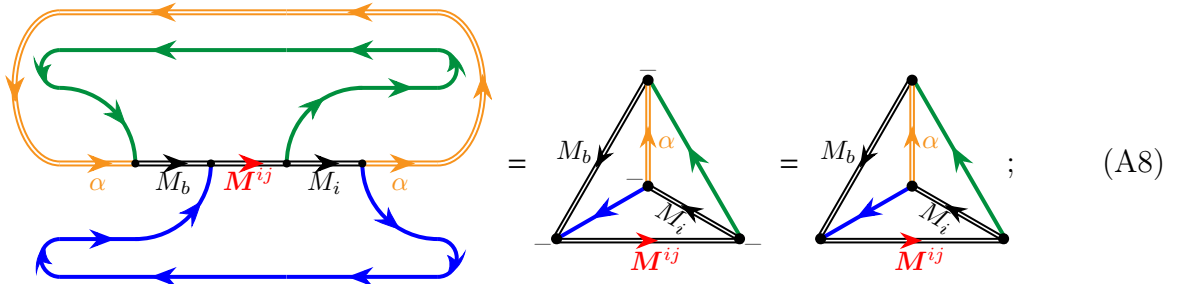
$$= \sum_b \frac{d_b}{M_b} \text{ (triangle diagram) } \cdot \text{ (horizontal line diagram) } . \quad (\text{A6})$$

Let us now take the trace of this equation: the left-hand side yields a product of $3j$ symbols,



$$= \frac{M_i}{d_i} \text{ (circle diagram) } , \quad (\text{A7})$$

while the trace of the birdtrack on the right-hand side gives us yet another $6j$ symbol,



$$= \text{ (triangle diagram) } = \text{ (triangle diagram) } ; \quad (\text{A8})$$

we were able to ignore the bars on all vertices as we assume that all representations meeting in any particular vertex are distinct, cf. Equation (18) (special cases not obeying this property are discussed separately in Appendix D).

Putting all of these pieces together, the trace of Equation (A6) amounts to the following

expression,

$$\frac{\text{circle}(M_i, M^{ij})}{d_i} \cdot \text{circle}(M_i, \alpha) = \sum_b \frac{d_b}{\text{circle}(M_b, \alpha) \cdot \text{circle}(M_b, M^{ij})} \cdot \underbrace{\text{triangle}(M_i, M_b, M^{ij}, \alpha)}_{S_{i,b}^{ij} S_{b,i}^{ij} = (S_{i,b}^{ij})^2} . \quad (\text{A9})$$

Since we are allowed to set all the $3j$ symbols simultaneously to 1, this reduces to

$$1 = d_i \sum_b d_b (S_{ib}^{ij})^2 . \quad (\text{A10})$$

Now, since M^{ij} is fixed, the only way for the $6j$ symbol $S_{i,b}^{ij}$ to be nonzero is if $b \in \{i, j\}$ (cf. Equation (13)). Hence, the sum on the right-hand side in Equation (A10) only has two terms, leaving us with the desired relation (26a),

$$1 = (d_i)^2 (S_{i,i}^{ij})^2 + d_i d_j (S_{i,j}^{ij})^2 . \quad (\text{A11})$$

b. Proof of Equation (26b): In an analogous way in which we built up the diagram in Equation (A1), let us now consider the diagram

$$\text{line}(\alpha, M_j, M^{ij}, M^{ij}, M_j) , \quad (\text{A12})$$

such that $i \neq j$ — in other words M_i and M_j label *inequivalent* irreps. Similarly to what we did in Equation (A6), let us take the Hermitian conjugate of (A12) and multiply it onto Equation (A4) from the right-hand side,

$$\text{line}(\alpha, M_j, M^{ij}, M^{ij}, M_j) \cdot \text{line}(\alpha, M_i, M^{ij}, M_j, \alpha) = \sum_b \frac{d_b}{\text{circle}(M_b, \alpha) \cdot \text{circle}(M_b, M^{ij})} \cdot \text{triangle}(M_i, M_b, M^{ij}, \alpha) \cdot \text{line}(\alpha, M_b, M^{ij}, M_j, \alpha) . \quad (\text{A13})$$

Again, we will take the trace of this equation: Since $i \neq j$ (that is M_i and M_j label inequivalent irreps), the left-hand side vanishes,

$$= 0 . \quad (\text{A14})$$

The trace of the birdtrack on the right-hand side once again gives us a $6j$ symbol,

$$= \frac{(22)}{(18)} \cdot \quad (\text{A15})$$

Putting all of the pieces together, we obtain the following relation,

$$0 = \sum_b \frac{d_b}{S_{i,b}^{ij} S_{b,j}^{ij}} \cdot \quad (\text{A16})$$

We will again set the $3j$ symbols to 1 such that this equation becomes

$$0 = \sum_b d_b S_{i,b}^{ij} S_{b,j}^{ij} . \quad (\text{A17})$$

Recalling that, since M^{ij} is fixed, the only way for the $6j$ symbols to be nonzero is if $b \in \{i, j\}$ in accordance with Equation (13). Therefore, the sum in Equation (A17) again only has two terms, leaving us with the desired result,

$$0 = d_i S_{i,i}^{ij} S_{i,j}^{ij} + d_j S_{i,j}^{ij} S_{j,j}^{ij} . \quad (\text{A18})$$

2. Proof of Equation (26c)

Let α be a particular Young diagram and let M_i and M_j be obtained from α by adding a box to row i and j , respectively (in accordance with Section III). Then, we may consider the following birdtrack diagram,

$$\text{Diagram (A19)} \quad . \quad (A19)$$

We may now insert a completeness relation between M_i and the green (top) quark-line to obtain

$$\text{Diagram (A19)} = \sum_{M^{ab}} \frac{d_{ab}}{\text{Diagram (A20)}} \quad (A20)$$

On the right hand side of this equation we obtain a $6j$ symbol from the vertex correction,

$$\text{Diagram (A21)} = \frac{1}{M_j} \text{Diagram (A21)} \quad (A21)$$

such that Equation (A20) reduces to

$$= \sum_{M^{ab}} \frac{d_{ab}}{M_i M_j} \text{ (triangle diagram) } \cdot \text{ (birdtrack diagram) } . \quad (\text{A22})$$

Let us now take the trace of Equation (A22): When tracing the birdtrack diagram on the left-hand side, we simply get a product of $3j$ symbols with a dimension factor,

$$= \frac{\alpha}{d_\alpha} \text{ (circular diagram) } . \quad (\text{A23})$$

The trace of the birdtrack on the right-hand side of Equation (A22) yields another $6j$ symbol,

$$= \text{ (triangle diagram) } . \quad (\text{A24})$$

Substituting expressions (A23) and (A24) back into the traced Equation (A22) yields

$$\frac{\text{Diagram}(M_j, \alpha)}{d_\alpha} \cdot \text{Diagram}(M_i, \alpha) = \sum_{M^{ab}} \frac{d_{ab}}{\text{Diagram}(M_i, M_j, M^{ab}) \cdot \text{Diagram}(M_j, M_i, M^{ab})}, \quad (\text{A25})$$

where we used Equation (24) to write $S_{j,i}^{ab} S_{i,j}^{ab} = (S_{i,j}^{ab})^2$ ($6j$ s for which this relation does not hold are discussed separately in Appendix D). We once again use the fact that we may set all the $3j$ symbols simultaneously to 1 to finally obtain the desired Equation (26c),

$$\frac{1}{d_\alpha} = \sum_{M^{ab}} d_{ab} (S_{i,j}^{ab})^2, \quad (\text{A26})$$

again with the only exception of $6j$ -symbols involving the antisymmetric vertex in eq. (17).

3. Proof of the linear relation Equation (26d)

Let M_i be a particular Young diagram obtained from α by adding a single box, and consider the following birdtrack diagram

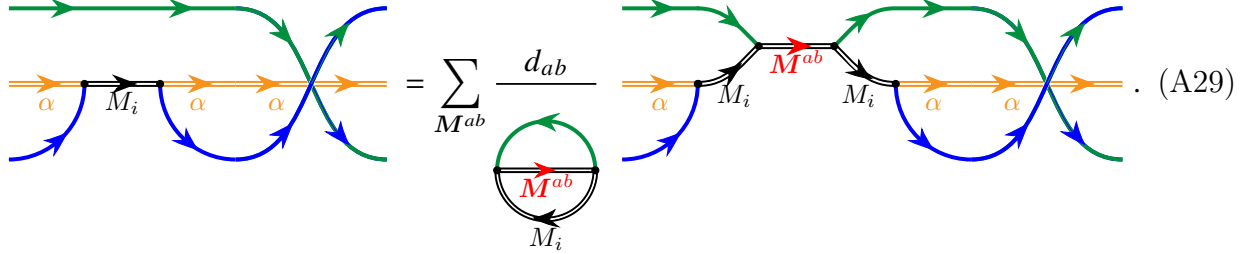
$$\text{Diagram}(\alpha, M_i, \alpha) \cdot \text{Diagram}(\text{Green line}) \quad (\text{A27})$$

Let us now insert a completeness relation (cf. Equation (6)) between M_i and the green (top) quark-line,

$$\text{Diagram}(\alpha, M_i, \alpha) \cdot \text{Diagram}(\text{Green line}) = \sum_{M^{ab}} \frac{d_{ab}}{\text{Diagram}(M_i, M^{ab}) \cdot \text{Diagram}(\text{Green lines}, M_i, M^{ab})} \quad (\text{A28})$$

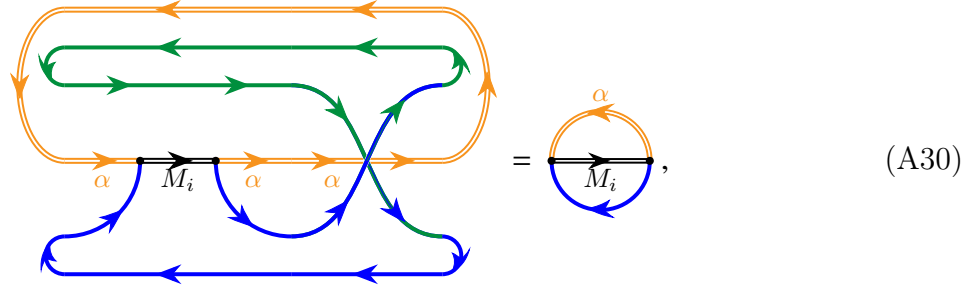
If we were to take a trace of this equation, we would obtain a bunch of $3j$ symbols, which is not particularly interesting. However, instead of merely taking a trace, let us first “swap”

the two quark-lines (i.e. we multiply Equation (A28) with a transposition between the two quark-lines from the right). This is a perfectly legal thing to do as the two quark-lines are both in the fundamental representation by definition,



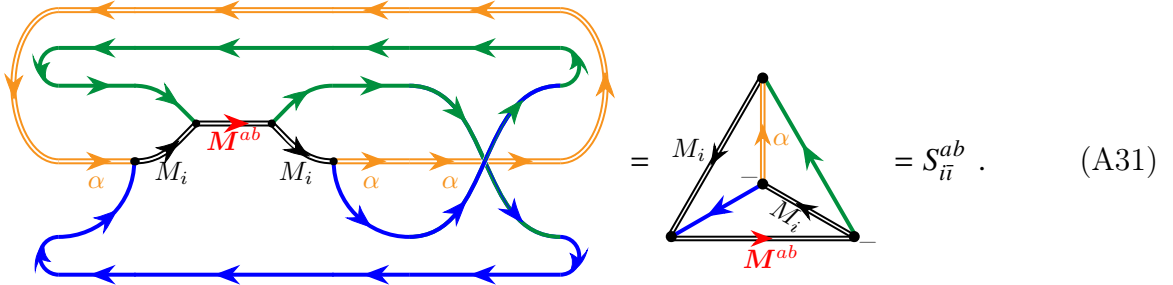
$$\text{Diagram} = \sum_{M^{ab}} \frac{d_{ab}}{\text{Diagram}} \cdot \text{Diagram} \quad (\text{A29})$$

If we now take the trace of this equation, the left-hand side will still yield a $3j$ symbol,



$$\text{Diagram} = \text{Diagram} \quad (\text{A30})$$

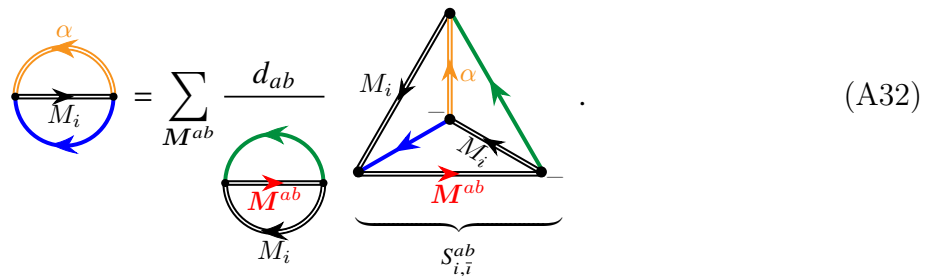
but the right-hand side yields a $6j$ symbol,



$$\text{Diagram} = \text{Diagram} = S_{i, \bar{i}}^{ab} \quad (\text{A31})$$

The symbol $S_{i, \bar{i}}^{ab}$ is similar to the $6j$ symbol $S_{i, i}^{ab}$, except the bar over one of the indices, \bar{i} , indicates that the vertices adjacent to one representation line M_i have been conjugated.

Putting the pieces together, we find that



$$\text{Diagram} = \sum_{M^{ab}} \frac{d_{ab}}{\text{Diagram}} \cdot \text{Diagram} = S_{i, \bar{i}}^{ab} \quad (\text{A32})$$

Once again, we ignore the conjugated vertices on the $6j$ symbol $S_{i,\bar{i}}^{ab}$ as we assume that Equation (18) holds, and refer the reader to Appendix D for all $6j$ symbols for which the assumption (18) is not valid. Thus, we have that $S_{i,\bar{i}}^{ab} = S_{i,i}^{ab}$, and Equation (A32) reduces to

The diagram shows the decomposition of a 6j symbol. On the left, a circular diagram with a horizontal line through the center. The top half is an orange arc with an arrow pointing right, labeled α . The bottom half is a blue arc with an arrow pointing left, labeled M_i . This is equal to a sum over M^{ab} of $\frac{d_{ab}}{M_i}$ multiplied by a triangle diagram. The triangle has three vertices. The top vertex has an orange arrow pointing up, labeled α . The bottom-left vertex has a blue arrow pointing left, labeled M_i . The bottom-right vertex has a red arrow pointing right, labeled M^{ab} . The bottom edge of the triangle is labeled $S_{i,i}^{ab}$.

Lastly, setting all $3j$ symbols to 1, we obtain the desired Equation (26d),

$$1 = \sum_b d_{ib} S_{i,i}^{ib}, \quad (\text{A34})$$

where we used the fact that at least one of the indices a, b (which one doesn't matter due to Equation (9)) must be equal to i for the $6j$ symbol to be nonzero, cf. Equation (15).

Appendix B: Fixing the sign ambiguity

In this section, we will determine the signs for the $6j$ symbols $S_{i,i}^{ii}$, $S_{i,j}^{ij}$ and $S_{i,i}^{ij} = -\frac{d_j}{d_i} S_{j,j}^{ij}$ in Appendices B 1 to B 3, respectively. For the first two cases ($S_{i,i}^{ii}$ and $S_{i,j}^{ij}$), the overall sign can be determined in an N -independent way. For the last case ($S_{i,i}^{ij} = -\frac{d_j}{d_i} S_{j,j}^{ij}$) we are able to determine the signs uniquely for $N \leq 3$, but argue that further work is needed to reliably determine the signs for $N > 3$.

1. Fixing the sign of $S_{i,i}^{ii}$

We start by determining the sign of $S_{i,i}^{ii}$: Let us now recall that, by the definition of the $6j$ symbols given in Section III, i denotes the row of α at the end of which the new box was added. In particular, this means that the two boxes were added to the *same* row for the symbol $S_{i,i}^{ii}$, implying that the two quark-lines enter symmetrically in M^i . Let us now

re-draw the $6j$ symbol somewhat:

$$S_{i,i}^{ii} = M_i \begin{array}{c} \text{triangle with } \alpha \text{ and } M_i \text{ lines} \end{array} = M_i \begin{array}{c} \text{square with } \alpha \text{ and } M_i \text{ lines} \end{array} \stackrel{(18)}{=} M_i \begin{array}{c} \text{square with } \alpha \text{ and } M_i \text{ lines} \end{array}. \quad (\text{B1})$$

Rewriting the crossed fundamental lines in the last birdtrack as a sum of symmetrizers and antisymmetrizers, $\begin{array}{c} \diagup \\ \diagdown \end{array} = \begin{array}{c} \left[\begin{array}{c} \leftarrow \\ \rightarrow \end{array} \right] - \begin{array}{c} \left[\begin{array}{c} \rightarrow \\ \leftarrow \end{array} \right] \end{array}$ (see, for example, Ref. 36), we obtain

$$S_{i,i}^{ii} = M_i \begin{array}{c} \text{square with } \alpha \text{ and } M_i \text{ lines} \end{array} = M_i \begin{array}{c} \text{square with } \alpha \text{ and } M_i \text{ lines} \end{array} - M_i \begin{array}{c} \text{square with } \alpha \text{ and } M_i \text{ lines} \end{array}. \quad (\text{B2})$$

Since the two quark-lines enter symmetrically in M^{ii} , the last term in Equation (B2) vanishes. More precisely, rewriting the triple product $\alpha \otimes \square \otimes \square$ as $(\alpha \otimes \square \square) \oplus (\alpha \otimes \begin{array}{c} \square \\ \square \end{array})$ and decomposing the result into irreps, one can check that M^{ii} appears in $\alpha \otimes \square \square$ but not in $\alpha \otimes \begin{array}{c} \square \\ \square \end{array}$. Thus, writing $\begin{array}{c} \left[\begin{array}{c} \leftarrow \\ \rightarrow \end{array} \right] = \frac{1}{2} \left(\begin{array}{c} \leftarrow \\ \leftarrow \end{array} + \begin{array}{c} \diagup \\ \diagdown \end{array} \right)$,

$$S_{i,i}^{ii} = M_i \begin{array}{c} \text{square with } \alpha \text{ and } M_i \text{ lines} \end{array} = \frac{1}{2} \left(M_i \begin{array}{c} \text{square with } \alpha \text{ and } M_i \text{ lines} \end{array} + M_i \begin{array}{c} \text{square with } \alpha \text{ and } M_i \text{ lines} \end{array} \right). \quad (\text{B3})$$

Recognizing the second term of the right-hand side as $\frac{1}{2} S_{i,i}^{ii}$ and taking it to the left-hand side, we notice that the right-hand side reduces to a product of $3j$ symbols with a dimension factor,

$$S_{i,i}^{ii} = M_i \begin{array}{c} \text{square with } \alpha \text{ and } M_i \text{ lines} \end{array} = M_i \begin{array}{c} \text{square with } \alpha \text{ and } M_i \text{ lines} \end{array} = \frac{M_i}{d_i} \cdot \begin{array}{c} \text{two } 3j \text{ symbols} \end{array}. \quad (\text{B4})$$

Again setting the $3j$ symbols to 1, we obtain that

$$S_{i,i}^{ii} = \frac{1}{d_i}, \quad (\text{B5})$$

now with a definite sign. We comment that, in determining the sign of $S_{i,i}^{ii}$, we actually rederived $S_{i,i}^{ii}$ with a definite sign. However, since similar methods will not work for $S_{i,j}^{ii}$, $S_{i,j}^{jj}$, and $S_{i,j}^{ij}$, we view this as a consistency check and continue to use Equations (26) to derive the functional forms of the remaining $6j$ symbols.

2. Fixing the sign of $S_{i,j}^{ij}$ for $i \neq j$

Consider the graphical notation for $S_{i,j}^{ij}$,

$$S_{i,j}^{ij} = \begin{array}{c} \begin{array}{ccc} & 4 & \\ & \uparrow \alpha & \\ & 1 & \\ \begin{array}{c} M_i \\ \nearrow \end{array} & & \begin{array}{c} \searrow \\ M_j \end{array} \\ 3 & & 2 \\ \begin{array}{c} \nearrow \\ M_j \end{array} & & \begin{array}{c} \searrow \\ M_i \end{array} \\ & & \begin{array}{c} \leftarrow \\ M^{ij} \end{array} \end{array} \end{array} \quad (B6)$$

Notice that each vertex occurs exactly once in this $6j$ symbol,

$$\begin{array}{c} \begin{array}{c} \uparrow \alpha \\ 1 \\ \begin{array}{c} \nearrow \\ M_j \end{array} \\ \begin{array}{c} \searrow \\ M_i \end{array} \end{array} \quad , \quad \begin{array}{c} \begin{array}{c} \uparrow \\ 2 \\ \begin{array}{c} \nearrow \\ M^{ij} \end{array} \\ \begin{array}{c} \searrow \\ M_j \end{array} \end{array} \quad , \quad \begin{array}{c} \begin{array}{c} \uparrow \\ 3 \\ \begin{array}{c} \nearrow \\ M_i \end{array} \\ \begin{array}{c} \searrow \\ M^{ij} \end{array} \end{array} \quad , \quad \begin{array}{c} \begin{array}{c} \uparrow \alpha \\ 4 \\ \begin{array}{c} \nearrow \\ M_i \end{array} \\ \begin{array}{c} \searrow \\ M_j \end{array} \end{array} \end{array} \quad (B7)$$

The overall sign of the $6j$ symbol $S_{i,j}^{ij}$ is uniquely determined by how one decided to define the vertices that occur in this $6j$ symbol. When iteratively computing these $6j$ symbols, starting with small Young diagrams and then adding more and more boxes, we may encounter vertices that were already used for earlier $6j$ s. If all four vertices have been encountered earlier then the sign of the $6j$ symbol may already be fixed. Otherwise we can pick the sign of the $6j$ to be, say, positive, thus imposing a constraint on signs of the vertices. Often a pair of vertices (either vertices 1 and 4 or vertices 2 and 3) is encountered for the first time in the $6j$ symbol to compute. Then, picking the sign of the $6j$ puts a constraint on the product of the signs of the newly encountered vertex pair. Since fully contracted color structures consist of dimensions, $3j$ symbols and $6j$ symbols *only*, the information used and obtained in an iterative computation of $6j$ symbols is sufficient to perform calculations in color space.

3. Fixing the sign of $S_{i,i}^{ij}$ for $i \neq j$ (equivalently $S_{j,j}^{ij}$)

Lastly, we turn to the $6j$ symbols $S_{i,i}^{ij}$ and, equivalently, $S_{j,j}^{ij}$, whose functional form is given in [Theorem 1](#). We notice that, for these $6j$ symbols, each vertex occurs together with its complex conjugated version. Thus, merely the vertex definitions do not determine the overall sign but a different method has to be chosen.

In the present section we will discuss how the linear relation [\(26d\)](#) can be used to fix the signs of $S_{i,i}^{ij}$ and $S_{j,j}^{ij}$ for $N \leq 3$, and comment on why additional work is needed to reliably fix the signs beyond $N = 3$. However, since our focus lies on physics applications (which will be discussed in a future paper), it is sufficient to fix the signs for $N = 3$, where N is interpreted as the number of colors N_c .

We require two preliminary results:

Lemma 1 (Determining the relative signs in a sum) *Consider the set of known, positive, real numbers $\{A_i\}_{i=1}^k$, and suppose that*

$$\sum_{i=1}^k \chi_i A_i = C , \quad (\text{B8})$$

where $C \in \mathbb{R} \setminus \{0\}$ is also known, and the $\chi_i \in \{-1, 1\}$ are to be determined. Then, if all subsets of $\{A_i\}_{i=1}^k$ satisfy

$$\sum_{l=1}^{m \leq k} \chi_{j_l} A_{j_l} \neq 0 , \quad (\text{B9})$$

all the χ_i can be determined uniquely.

Proof of Lemma 1. We present a proof by contradiction: Let the $\{A_i\}_{i=1}^k$ be such that conditions [\(B8\)](#) and [\(B9\)](#) laid out in the lemma are satisfied. Suppose now that [Equation \(B8\)](#) does not uniquely determine all the $\chi_i \in \{-1, 1\}$, that is, there exist some $\{j_1, \dots, j_m\} \subset \{1, \dots, k\}$ such that

$$\sum_{i \in \{1, \dots, k\} \setminus \{j_1, \dots, j_m\}} \chi_i A_i + \sum_{i \in \{j_1, \dots, j_m\}} \chi_i A_i = C \quad (\text{B10a})$$

and

$$\sum_{i \in \{1, \dots, k\} \setminus \{j_1, \dots, j_m\}} \chi_i A_i - \sum_{i \in \{j_1, \dots, j_m\}} \chi_i A_i = C . \quad (\text{B10b})$$

Then, deducting [Equation \(B10b\)](#) from [Equation \(B10a\)](#), we obtain

$$\sum_{i \in \{j_1, \dots, j_m\}} \chi_i A_i = 0 . \quad (\text{B11})$$

Thus, we have found a partial sum of the products $\chi_i A_i$ that vanishes, which poses a contradiction to [Equation \(B9\)](#). \square

Lemma 2 (Adding a box to the first row of a Young diagram) *Let α be a Young diagram and let M_1 and M^{11} be the diagrams obtained from α by adding one, respectively two, box(es) to the first row of α . Furthermore, let d_1 and d_{11} be the dimensions of the irreducible representations corresponding to M_1 and M^{11} , respectively. Then,*

$$\frac{d_{11}}{d_1} = 1 \quad \Rightarrow \quad N \leq 1 , \quad (\text{B12})$$

where equality holds if and only if α is the totally symmetric diagram consisting of exactly one row.

Proof of Lemma 2. Let $h_{a,b}$ be the hook lengths (see [Appendix E](#)) of α , and denote by ℓ the length of α 's first row. We calculate d_{11}/d_1 using the factors-over-hooks formula [\(E2\)](#). For M^{11} , compared to M_1 , we obtain just one additional factor, namely $N + \ell + 1$ for the last box in the first row, and only the hook lengths for the boxes in the first row differ. In the quotient d_{11}/d_1 all other hook lengths cancel, i.e.

$$\frac{d_{11}}{d_1} = (N + \ell + 1) \frac{(h_{1,1} + 1)(h_{1,2} + 1) \cdots (h_{1,\ell} + 1) \cdot 1}{(h_{1,1} + 2)(h_{1,2} + 2) \cdots (h_{1,\ell} + 2) \cdot 2} . \quad (\text{B13})$$

Hence,

$$d_{11}/d_1 = 1 \quad \Leftrightarrow \quad N = \frac{(h_{1,1} + 2)(h_{1,2} + 2) \cdots (h_{1,\ell} + 2)}{(h_{1,1} + 1)(h_{1,2} + 1) \cdots (h_{1,\ell} + 1)} \cdot 2 - \ell - 1 . \quad (\text{B14})$$

The quotients $\frac{h_{1,b} + 2}{h_{1,b} + 1}$ are maximal if $h_{1,b}$ is minimal, and $h_{1,b} \geq \ell - b + 1$, where equality holds if and only if there is only one box in column b . Therefore,

$$N \leq \frac{(\ell + 2)(\ell + 1) \cdots 3}{(\ell + 1) \cdots 3 \cdot 2} \cdot 2 - \ell - 1 = 1 , \quad (\text{B15})$$

as required. \square

Let's manipulate the linear relation [\(26d\)](#) a little bit: First, we single out the known value $S_{i,i}^{ii} = \frac{1}{d_i}$ from the sum,

$$1 = \sum_b d_{ib} S_{i,i}^{ib} = \frac{d_{ii}}{d_i} + \sum_{b \neq i} d_{ib} S_{i,i}^{ib} . \quad (\text{B16})$$

We would like to view the signs of the $6j$ symbols as variables to be determined, and therefore define χ_{ij}

$$\chi_{ij} = \chi_{ji} \in \{-1, 1\}, \quad (\text{B17})$$

such that

$$S_{i,i}^{ij} = \chi_{ij} \frac{1}{d_i} \sqrt{1 - \frac{d_i d_j}{d_\alpha d_{ij}}}. \quad (\text{B18})$$

Notice that χ_{ij} does *not* encompass the relative sign between $S_{i,i}^{ij}$ and $S_{j,j}^{ji}$, but denotes the *absolute* sign of $S_{i,i}^{ij}$. In other words,

$$S_{i,i}^{ij} = \chi_{ij} \frac{1}{d_i} \sqrt{1 - \frac{d_i d_j}{d_\alpha d_{ij}}} \stackrel{(32)}{=} -\chi_{ij} \frac{1}{d_j} \sqrt{1 - \frac{d_i d_j}{d_\alpha d_{ij}}} = -\frac{d_j}{d_i} S_{j,j}^{ji}. \quad (\text{B19})$$

Furthermore, to make the notation a bit shorter, let us define the symbol A_{ij} as

$$A_{ij} = \frac{d_{ij}}{d_i} \sqrt{1 - \frac{d_i d_j}{d_\alpha d_{ij}}} \implies \chi_{ij} A_{ij} = d_{ij} S_{i,i}^{ij}. \quad (\text{B20})$$

Clearly, the d_{ij} are symmetric in i and j , and so are the $S_{i,i}^{ij}$ in their upper indices by Equation (9), $S_{i,i}^{ij} = S_{i,i}^{ji}$. However, $S_{i,i}^{ij}$ and $S_{j,j}^{ji}$ are related by a negative pre-factor according to Equation (32) in Theorem 1, such that the A_{ij} are antisymmetric,

$$A_{ji} = -A_{ij}. \quad (\text{B21})$$

Then, taking $\frac{d_{ii}}{d_i}$ to the other side of the equal sign and implementing notation (B20), the linear equations in (B16) can be cast into matrix form,

$$\begin{pmatrix} 0 & \chi_{12} A_{12} & \chi_{13} A_{13} & \cdots & \chi_{1N} A_{1N} \\ -\chi_{12} A_{12} & 0 & \chi_{23} A_{23} & \cdots & \chi_{2N} A_{2N} \\ -\chi_{13} A_{13} & -\chi_{23} A_{23} & 0 & \cdots & \chi_{3N} A_{3N} \\ \vdots & \vdots & \vdots & \ddots & \vdots \\ -\chi_{1N} A_{1N} & -\chi_{2N} A_{2N} & -\chi_{3N} A_{3N} & \cdots & 0 \end{pmatrix} \begin{pmatrix} 1 \\ 1 \\ 1 \\ \vdots \\ 1 \end{pmatrix} = \begin{pmatrix} 1 - \frac{d_{11}}{d_1} \\ 1 - \frac{d_{22}}{d_2} \\ 1 - \frac{d_{33}}{d_3} \\ \vdots \\ 1 - \frac{d_{NN}}{d_N} \end{pmatrix}. \quad (\text{B22})$$

Recall that the A_{ij} are known (as the dimensions d_α , d_i , d_j and d_{ij} are known, cf. Equation (B20)) and that we seek to determine the $\chi_{ij} \in \{-1, 1\}$ for each pair (i, j) . We shall denote the linear equation resulting from row r of the matrix equation (B22) by $E(r)$, that is:

$$E(r) : -\sum_{i=1}^{r-1} \chi_{ir} A_{ir} + \sum_{j=r+1}^N \chi_{rj} A_{rj} = 1 - \frac{d_{rr}}{d_r}. \quad (\text{B23})$$

Notice that, up to this point, we have not specified a particular value for N but kept the discussion fully general. From now on, let us fix $N = 3$. (We note that the below argument also works for $N < 3$. At the end of this section, we comment on why the strategy presented here for determining the signs breaks down for $N > 3$.)

a. For $N = 3$, the matrix equation (B22) simplifies as

$$\begin{pmatrix} 0 & \chi_{12}A_{12} & \chi_{13}A_{13} \\ -\chi_{12}A_{12} & 0 & \chi_{23}A_{23} \\ -\chi_{13}A_{13} & -\chi_{23}A_{23} & 0 \end{pmatrix} \begin{pmatrix} 1 \\ 1 \\ 1 \end{pmatrix} = \begin{pmatrix} 1 - \frac{d_{11}}{d_1} \\ 1 - \frac{d_{22}}{d_2} \\ 1 - \frac{d_{33}}{d_3} \end{pmatrix}. \quad (\text{B24})$$

From Lemma 2 we know that $\frac{d_{11}}{d_1} \neq 1$ for all $N > 1$, so, in particular, also for $N = 3$. Therefore, the right-hand side of $E(1)$ is nonzero, which means that

$$A_{12} \neq A_{13} \quad \text{and} \quad \text{not both } A_{12} \text{ and } A_{13} \text{ are zero.} \quad (\text{B25})$$

We distinguish two cases:

1. If $A_{12} \neq 0$ and $A_{13} \neq 0$, then both χ_{12} and χ_{13} can be determined uniquely from $E(1)$ by Lemma 1.
 - (a) If $A_{23} \neq 0$, we may also uniquely determine χ_{23} .
 - (b) If $A_{23} = 0$ for $N = 3$, the corresponding $6j$ symbols S_{22}^{23} and S_{33}^{23} both vanish and hence χ_{23} is irrelevant.
2. If only one of A_{12} and A_{13} is nonzero (i.e. only one of χ_{12} and χ_{13} can be determined uniquely), this means that the other $6j$ symbol is zero, making the corresponding χ_{ij} irrelevant. Without loss of generality, suppose that χ_{12} is uniquely determinable and hence $S_{11}^{13} = 0 = S_{33}^{13}$ (the analogous argument can be made if only χ_{13} is uniquely determinable).
 - (a) If $A_{23} \neq 0$, we may also uniquely determine χ_{23} from $E(2)$ using our result for χ_{12} .
 - (b) If $A_{23} = 0$, the corresponding $6j$ symbols S_{22}^{23} and S_{33}^{23} both vanish, making χ_{23} irrelevant.

Therefore, for $N = 3$ all signs of the nonzero $6j$ symbols are uniquely determinable.

Let us briefly comment on possibly non-existing $6j$ symbols: Notice that, for a particular diagram α , boxes may be added only to the second row but not the third row (or vice versa), implying that the $6j$ symbols with an index 3 (resp. 2) do not exist. Examples of these are

$$\alpha = \begin{array}{|c|c|c|} \hline \square & \square & \square \\ \hline \square & \square & \square \\ \hline \square & \square & \square \\ \hline \end{array} \longrightarrow \text{boxes can only be added in rows 1 and 2} \quad (\text{B26a})$$

$$\alpha = \begin{array}{|c|c|} \hline \square & \square \\ \hline \square & \square \\ \hline \square & \square \\ \hline \end{array} \longrightarrow \text{boxes can only be added in rows 1 and 3.} \quad (\text{B26b})$$

Then, in both cases, the matrix equation (B24) reduces to something even simpler, namely

$$\begin{pmatrix} 0 & \chi_{1j}A_{1j} \\ -\chi_{1j}A_{1j} & 0 \end{pmatrix} \begin{pmatrix} 1 \\ 1 \end{pmatrix} = \begin{pmatrix} 1 - \frac{d_{11}}{d_1} \\ 1 - \frac{d_{jj}}{d_j} \end{pmatrix} \quad \text{where } j = 2 \text{ (resp. } j = 3) \text{,} \quad (\text{B27})$$

and hence the signs of the only remaining $6j$ symbols S_{11}^{1j} and S_{jj}^{1j} can be determined from the sign of $1 - \frac{d_{11}}{d_1} \neq 0$.

b. Going beyond $N = 3$: Notice that for $N = 3$, each equation $E(n)$ has exactly $N - 1 = 2$ terms on the left-hand side. Since the right-hand side of $E(1)$ is non-zero for all values of N , this, in particular, allows us to uniquely determine the sign of both terms of $E(1)$ for $N = 3$, and thus also for one of the two terms appearing on the left-hand sides of $E(2)$ and $E(3)$, respectively. This is no longer the case for $N > 3$ as the left hand-sides of equations $E(n)$ contain $N - 1 > 2$ terms, and further information is needed to uniquely determine their signs.

Appendix C: Vertex properties

We discuss the behavior of vertices under line swapping. Consider three irreps α , β and γ with $\gamma^* \subset \alpha \otimes \beta$. For each instance of γ^* in $\alpha \otimes \beta$ we introduce — for the sake of argument — two vertices

$$\begin{array}{c} \alpha \\ \swarrow \quad \searrow \\ \bullet \\ \downarrow \gamma \\ \beta \end{array} \quad \text{and} \quad \begin{array}{c} \beta \\ \swarrow \quad \searrow \\ \bullet \\ \downarrow \gamma \\ \alpha \end{array}, \quad (\text{C1})$$

which differ by line ordering (and possibly other “internal” vertex structure). If the multiplicity of γ^* in $\alpha \otimes \beta$ is one (or, equivalently, if the multiplicity of β^* in $\alpha \otimes \gamma$ is one or, equivalently, if the multiplicity of α^* in $\beta \otimes \gamma$ is one), then the two vertices must be proportional

$$\begin{array}{c} \alpha \\ \swarrow \quad \searrow \\ \bullet \\ \downarrow \gamma \\ \beta \end{array} = c \begin{array}{c} \beta \\ \swarrow \quad \searrow \\ \bullet \\ \downarrow \gamma \\ \alpha \end{array}, \quad (\text{C2})$$

with some non-zero a priori complex constant c . All vertices appearing in this work have multiplicity one, as can be seen from Young diagram multiplication, using that in each vertex at least one line is in the fundamental representation.

Next, we consider the complex conjugates of both vertices, and temporarily introduce different symbols for them,

$$\left(\begin{array}{c} \alpha \quad \beta \\ \nearrow \quad \nwarrow \\ \bullet \\ \downarrow \gamma \end{array} \right)^* = \begin{array}{c} \alpha \quad \beta \\ \nwarrow \quad \nearrow \\ \bullet \\ \downarrow \gamma \end{array} \quad \text{and} \quad \left(\begin{array}{c} \beta \quad \alpha \\ \nwarrow \quad \nearrow \\ \circ \\ \downarrow \gamma \end{array} \right)^* = \begin{array}{c} \beta \quad \alpha \\ \nearrow \quad \nwarrow \\ \circ \\ \downarrow \gamma \end{array}. \quad (\text{C3})$$

The complex conjugate of Equation (C2) reads

$$\begin{array}{c} \beta \quad \alpha \\ \nwarrow \quad \nearrow \\ \circ \\ \downarrow \gamma \end{array} = c^* \begin{array}{c} \beta \quad \alpha \\ \nearrow \quad \nwarrow \\ \bullet \\ \downarrow \gamma \end{array}, \quad (\text{C4})$$

and we can use these two equations in order to relate two $3j$ symbols,

$$\begin{array}{c} \alpha \\ \nearrow \\ \bullet \\ \leftarrow \beta \\ \leftarrow \\ \circ \\ \rightarrow \gamma \\ \searrow \end{array} \stackrel{(\text{C2})}{=} c \begin{array}{c} \beta \\ \nwarrow \\ \circ \\ \leftarrow \alpha \\ \leftarrow \\ \bullet \\ \rightarrow \gamma \\ \searrow \end{array} \stackrel{(\text{C4})}{=} |c|^2 \begin{array}{c} \beta \\ \nwarrow \\ \bullet \\ \leftarrow \alpha \\ \leftarrow \\ \circ \\ \rightarrow \gamma \\ \searrow \end{array}. \quad (\text{C5})$$

If we normalize all $3j$ symbols in the same way (we prefer to set them to 1, but the argument also works for any other normalization) then we conclude that $|c| = 1$. In fact, if $\alpha \neq \beta \neq \gamma \neq \alpha$, we can, and do, always choose $c = 1$, which is the most natural choice.

However, if two of the three irreps meeting in a vertex are equivalent, say $\beta = \alpha$, then the two vertices defined in Equation (C1) are proportional to each other, and we make the natural choice

$$\begin{array}{c} \alpha \quad \alpha \\ \nwarrow \quad \nearrow \\ \bullet \\ \downarrow \gamma \end{array} = \begin{array}{c} \alpha \quad \alpha \\ \nearrow \quad \nwarrow \\ \circ \\ \downarrow \gamma \end{array}, \quad (\text{C6})$$

any other choice would give a redundant definition. In this case Equation (C2) becomes

$$\begin{array}{c} \alpha \quad \alpha \\ \nwarrow \quad \nearrow \\ \circ \\ \downarrow \gamma \end{array} = c \begin{array}{c} \alpha \quad \alpha \\ \nearrow \quad \nwarrow \\ \bullet \\ \downarrow \gamma \end{array}, \quad (\text{C7})$$

and by intertwining the upper two lines in the last equation we also obtain

$$\begin{array}{c} \alpha \quad \alpha \\ \nearrow \quad \nwarrow \\ \bullet \\ \downarrow \gamma \end{array} = c \begin{array}{c} \alpha \quad \alpha \\ \nwarrow \quad \nearrow \\ \circ \\ \downarrow \gamma \end{array}. \quad (\text{C8})$$

Finally, dividing both sides with c , $c = \frac{1}{c}$, and we find $c = \pm 1$, i.e. we are left with a sign. In this work, the only irrep which can appear more than once in a vertex is the fundamental

representation, or, in other words, if two identical lines meet in a vertex then they are always quark-lines. Hence, there are only two vertices of this kind relevant for this work, one with $c = 1$ and one with $c = -1$,

$$\begin{array}{c} \text{---} \\ \text{---} \\ \text{---} \\ \square \end{array} = \begin{array}{c} \text{---} \\ \text{---} \\ \text{---} \\ \square \end{array} \quad \text{and} \quad \begin{array}{c} \text{---} \\ \text{---} \\ \text{---} \\ \square \end{array} = - \begin{array}{c} \text{---} \\ \text{---} \\ \text{---} \\ \square \end{array}, \quad (\text{C9})$$

warranting the use of the same symbol \bullet for all vertices.

From here on, we again use the same symbol \bullet for both vertices \blacklozenge and \blacksquare , and let the arrow direction determine which vertex is intended. We also no longer use the vertices \odot and \square but instead swap lines on the vertex \bullet . If an equation becomes more legible with two lines swapped in a vertex, we indicate this swapping of lines by a barred vertex (cf. [Section IV A](#)), i.e. we define

$$\begin{array}{c} \beta \\ \alpha \\ \gamma \end{array} \begin{array}{c} \text{---} \\ \text{---} \\ \text{---} \\ \square \end{array} = \begin{array}{c} \beta \\ \alpha \\ \gamma \end{array} \begin{array}{c} \text{---} \\ \text{---} \\ \text{---} \\ \square \end{array}, \quad (\text{C10})$$

and for the purpose of this work we only have to keep in mind that there is exactly one vertex, see [Equation \(C9\)](#), for which omitting a bar leads to a sign change.

Appendix D: Special cases for line ordering in vertices

In [Appendix C](#) we explained that we can largely ignore the line ordering in (barred) vertices of the $6j$ symbols, since for the $6j$ symbols we study most vertices connect three *distinct* irrep lines. The only exception are vertices with two incoming or two outgoing quark-lines, and among these vertices only the vertex

$$\begin{array}{c} \text{---} \\ \text{---} \\ \text{---} \\ \square \end{array} \quad (\text{D1})$$

is antisymmetric in the two quark-lines, see [Equation \(C9\)](#).

In order to have two incoming or two outgoing quark-lines in a vertex within the $6j$ symbols under investigation,

$$\begin{array}{c} \alpha \\ M_i \\ M_j \\ M^{ij} \end{array} \begin{array}{c} \text{---} \\ \text{---} \\ \text{---} \\ \square \end{array}, \quad (\text{D2})$$

α or M_i or M_j needs to be the fundamental representation, i.e. a quark-line.

If $\alpha = \square$ then M_i and M_j can be either $\square\square$ or \square , and the only $6j$ s of this kind with at least one antisymmetric vertex are

(D3)

which have all been explicitly discussed and calculated in Ref. 30.

If $M_i = \square$, then M^{ij} can be either $\square\square$ or \square , from which it follows that also $M_j = \square$, and α can be either the trivial representation (singlet) or the adjoint representation (a gluon-line). If α is a singlet then the $6j$ symbol, up to normalization, reduces to a $3j$ symbol. If α is the adjoint representation, then the only $6j$ of this kind with at least one antisymmetric vertex is

(D4)

which has also been calculated in Ref. 30; in fact, it also reduces, up to normalization, to a $3j$ by the Fierz identity.

Appendix E: Dimensions of Young diagrams

As is clear from [Theorem 1](#), calculating the dimensions of the irreps contained in a $6j$ is imperative to calculating the values of the $6j$ symbols discussed in this paper. Therefore, we here recapitulate how to calculate these dimensions directly from the corresponding diagrams.

First, we present the factors-over-hooks formula without proof; proofs can be found in standard textbooks such as Refs. [36,38,39](#).

Consider a Young diagram λ . For each of its cells, we may define a *factor* and a *hook length* in the following way:

- the *factor* $f_{a,b}$ of the cell $c_{a,b} \in \lambda$ in the a^{th} row and the b^{th} column is defined as

$$f_{a,b} = b - a . \tag{E1}$$

- the *hook length* $h_{a,b}$ of the cell $c_{a,b}$ is defined to be the number of cells to the right of $c_{a,b}$ plus the number of cells below $c_{a,b}$ plus 1 ($c_{a,b}$ itself).

Then, the dimension of the $SU(N)$ irrep corresponding to the diagram λ is given by

$$\dim(\lambda) = \prod_{c_{a,b} \in \lambda} \frac{(N + f_{a,b})}{h_{a,b}}, \quad (\text{E2})$$

where the product runs over all cells $c_{a,b}$ in λ . Let us provide an example for illustration:

Consider the Young diagram

$$\lambda = \begin{array}{cccc} \square & \square & \square & \square \\ \square & \square & & \\ \square & \square & & \\ \square & & & \end{array}. \quad (\text{E3})$$

Then, the factors and hook lengths of each of the cells are

$$\begin{array}{cc} \text{factors:} & \text{hook lengths:} \\ \begin{array}{|c|c|c|c|} \hline 0 & 1 & 2 & 3 \\ \hline -1 & 0 & & \\ \hline -2 & -1 & & \\ \hline -3 & & & \\ \hline \end{array} & \begin{array}{|c|c|c|c|} \hline 7 & 5 & 2 & 1 \\ \hline 4 & 2 & & \\ \hline 3 & 1 & & \\ \hline 1 & & & \\ \hline \end{array}, \quad (\text{E4}) \end{array}$$

such that the dimension of the irrep corresponding to λ is given by

$$\dim(\lambda) = \left[\frac{N(N+1)(N+2)}{7 \cdot 5 \cdot 2} (N+3) \right] \left[\frac{(N-1)N}{4 \cdot 2} \right] \left[\frac{(N-2)}{3} (N-1) \right] [N-3], \quad (\text{E5})$$

which is zero for $N \leq 3$ and, for example, becomes 36 for $N = 4$.

In QCD, a general Fock space sector may contain fundamental, antifundamental and also adjoint factors. Young diagrams for irreps on such a sector reflect this by containing the following conglomerates of boxes,

$$\begin{array}{ccc} \text{fundamental:} & \text{antifundamental:} & \text{adjoint:} \\ \square & \left. \begin{array}{|c|} \hline \square \\ \square \\ \vdots \\ \square \\ \hline \end{array} \right\} N-1 & \left. \begin{array}{|c|c|} \hline \square & \square \\ \square & \square \\ \vdots & \vdots \\ \square & \square \\ \hline \end{array} \right\} N-1 \\ \dim = N & \dim = N & \dim = N^2 - 1, \quad (\text{E6}) \end{array}$$

where the dimensions can be verified using the factors-over-hooks formula. For $SU(N)$, a column of length N may be crossed out in the calculation of the dimension (as the hook lengths in this column will cancel with the factors at the end of the respective rows), but it

may be preferable to not go the route of first adding boxes that will ultimately be taken away. King⁴⁰ offers such a way in terms of back-to-back tableaux, where columns of length $N - 1$ are represented as boxes that are added *to the left* of the given Young diagram. We will not review this method of multiplying diagrams and calculating the corresponding dimensions here but rather refer readers to the original source, Ref. 40.

REFERENCES

- ¹J. E. Paton and H.-M. Chan, “Generalized Veneziano model with isospin,” *Nucl. Phys. B* **10**, 516–520 (1969).
- ²F. A. Berends and W. Giele, “The six gluon process as an example of Weyl-van der Waerden spinor calculus,” *Nucl. Phys.* **B294**, 700 (1987).
- ³M. L. Mangano, S. J. Parke, and Z. Xu, “Duality and multi-gluon scattering,” *Nucl. Phys. B* **298**, 653 (1988).
- ⁴M. L. Mangano, “The color structure of gluon emission,” *Nucl. Phys. B* **309**, 461 (1988).
- ⁵D. A. Kosower, “Color factorization for fermionic amplitudes,” *Nucl. Phys.* **B315**, 391–418 (1989).
- ⁶Z. Nagy and D. E. Soper, “Parton showers with quantum interference,” *JHEP* **09**, 114 (2007), [arXiv:0706.0017 \[hep-ph\]](#).
- ⁷M. Sjödal, “Color structure for soft gluon resummation – a general recipe,” *JHEP* **0909**, 087 (2009), [arXiv:0906.1121 \[hep-ph\]](#).
- ⁸J. Alwall, M. Herquet, F. Maltoni, O. Mattelaer, and T. Stelzer, “MadGraph 5: going beyond,” *JHEP* **1106**, 128 (2011), [arXiv:1106.0522 \[hep-ph\]](#).
- ⁹M. Sjödal, “ColorFull – a C++ library for calculations in $SU(N_c)$ color space,” *Eur.Phys.J.* **C75**, 236 (2015), [arXiv:1412.3967 \[hep-ph\]](#).
- ¹⁰S. Plätzer and M. Sjödal, “Subleading N_c improved parton showers,” *JHEP* **1207**, 042 (2012), [arXiv:1201.0260 \[hep-ph\]](#).
- ¹¹S. Plätzer, M. Sjödal, and J. Thorén, “Color matrix element corrections for parton showers,” *JHEP* **11**, 009 (2018), [arXiv:1808.00332 \[hep-ph\]](#).
- ¹²G. ’t Hooft, “A planar diagram theory for strong interactions,” *Nucl. Phys.* **B72**, 461 (1974).
- ¹³A. Kanaki and C. G. Papadopoulos, “HELAC-PHEGAS: Automatic computation of

- helicity amplitudes and cross-sections,” *AIP Conf. Proc.* **583**, 169 (2002), [arXiv:hep-ph/0012004](#).
- ¹⁴F. Maltoni, K. Paul, T. Stelzer, and S. Willenbrock, “Color flow decomposition of QCD amplitudes,” *Phys. Rev. D* **67**, 014026 (2003), [arXiv:hep-ph/0209271 \[hep-ph\]](#).
- ¹⁵S. Plätzer, “Summing large- n towers in colour flow evolution,” *Eur. Phys. J. C* **74**, 2907 (2014), [arXiv:1312.2448 \[hep-ph\]](#).
- ¹⁶R. Ángeles Martínez, M. De Angelis, J. R. Forshaw, S. Plätzer, and M. H. Seymour, “Soft gluon evolution and non-global logarithms,” *JHEP* **05**, 044 (2018), [arXiv:1802.08531 \[hep-ph\]](#).
- ¹⁷M. De Angelis, J. R. Forshaw, and S. Plätzer, “Resummation and simulation of soft gluon effects beyond leading color,” *Phys. Rev. Lett.* **126**, 112001 (2021), [arXiv:2007.09648 \[hep-ph\]](#).
- ¹⁸S. Plätzer and I. Ruffa, “Towards colour flow evolution at two loops,” *JHEP* **06**, 007 (2021), [arXiv:2012.15215 \[hep-ph\]](#).
- ¹⁹S. Keppeler and M. Sjö Dahl, “Orthogonal multiplet bases in $SU(N_c)$ color space,” *JHEP* **09**, 124 (2012), [arXiv:1207.0609 \[hep-ph\]](#).
- ²⁰A. Kyrieleis and M. H. Seymour, “The colour evolution of the process $qq \rightarrow qqg$,” *JHEP* **01**, 085 (2006), [hep-ph/0510089](#).
- ²¹Y. L. Dokshitzer and G. Marchesini, “Soft gluons at large angles in hadron collisions,” *JHEP* **01**, 007 (2006), [arXiv:hep-ph/0509078](#).
- ²²M. Sjö Dahl, “Color evolution of $2 \rightarrow 3$ processes,” *JHEP* **12**, 083 (2008), [arXiv:0807.0555 \[hep-ph\]](#).
- ²³M. Beneke, P. Falgari, and C. Schwinn, “Soft radiation in heavy-particle pair production: All-order colour structure and two-loop anomalous dimension,” *Nucl. Phys. B* **828**, 69–101 (2010), [arXiv:0907.1443 \[hep-ph\]](#).
- ²⁴Y.-J. Du, M. Sjö Dahl, and J. Thorén, “Recursion in multiplet bases for tree-level MHV gluon amplitudes,” *JHEP* **05**, 119 (2015), [arXiv:1503.00530 \[hep-ph\]](#).
- ²⁵M. Sjö Dahl and J. Thorén, “Decomposing color structure into multiplet bases,” *JHEP* **09**, 055 (2015), [arXiv:1507.03814 \[hep-ph\]](#).
- ²⁶S. Keppeler and M. Sjö Dahl, “Hermitian Young operators,” *J. Math. Phys.* **55**, 021702 (2014), [arXiv:1307.6147 \[math-ph\]](#).
- ²⁷J. Alcock-Zeilinger and H. Weigert, “Simplification rules for birdtrack operators,” *J. Math.*

- Phys. **58**, 051701 (2017), arXiv:1610.08801.
- ²⁸J. Alcock-Zeilinger and H. Weigert, “Compact Hermitian Young projection operators,” *J. Math. Phys.* **58**, 051702 (2017), 1610.10088.
- ²⁹J. Alcock-Zeilinger and H. Weigert, “Transition operators,” *J. Math. Phys.* **58**, 051703 (2017), arXiv:1610.08802 [math-ph].
- ³⁰M. Sjodahl and J. Thorén, “QCD multiplet bases with arbitrary parton ordering,” *JHEP* **11**, 198 (2018), arXiv:1809.05002 [hep-ph].
- ³¹H. T. Johansson and C. Forssén, “Fast and accurate evaluation of Wigner $3j$, $6j$, and $9j$ symbols using prime factorization and multiword integer arithmetic,” *SIAM Journal on Scientific Computing* **38**, A376–A384 (2016).
- ³²A. Alex, M. Kalus, A. Huckleberry, and J. von Delft, “A numerical algorithm for the explicit calculation of $SU(n)$ and $SL(n, c)$ Clebsch-Gordan coefficients,” *Journal of Mathematical Physics* **52**, 023507 (2011).
- ³³T. Dytrych, D. Langr, J. P. Draayer, K. D. Launey, and D. Gazda, “SU3lib: A C++ library for accurate computation of Wigner and Racah coefficients of $SU(3)$,” *Comput. Phys. Commun.* **269**, 108137 (2021).
- ³⁴S. Gieseke, P. Kirchgaesser, S. Plätzer, and A. Siodmok, “Colour reconnection from soft gluon evolution,” *JHEP* **11**, 149 (2018), arXiv:1808.06770 [hep-ph].
- ³⁵S. Plätzer, “Colour evolution and infrared physics,” (2022), arXiv:2204.06956 [hep-ph].
- ³⁶P. Cvitanović, *Group theory: Birdtracks, Lie’s and exceptional groups* (Princeton Univ. Pr., USA: Princeton, 2008).
- ³⁷S. Keppeler, “Birdtracks for $SU(N)$,” *SciPost Phys. Lect. Notes* **3**, 1 (2018), arXiv:1707.07280 [math-ph].
- ³⁸W. Fulton, *Young Tableaux* (Cambridge Univ. Pr., UK: Cambridge, 1997).
- ³⁹B. E. Sagan, *The Symmetric Group - Representations, Combinatorial Algorithms, and Symmetric Functions*, 2nd ed. (Springer, USA: New York, 2000).
- ⁴⁰R. C. King, “Generalized Young tableaux and the general linear group,” *J. of Math. Phys.* **11**, 280–293 (1970).